08.1;13.1

Titanium Oxynitride Thin Films Wide Temperature Range Sensors

© F.A. Baron[1], L.V. Shanidze[1], M.V. Rautskiy[1], Yu.L. Mikhlin[2], A.V. Lukyanenko[1], S.O. Konovalov[3], F.V. Zelenov[3], P.V. Shvets[4], A.Yu. Goikhman[4], N.V. Volkov[1], A.S. Tarasov[1]

[1] Kirensky Institute of Physics, Federal Research Center KSC SB, Russian Academy of Sciences, Krasnoyarsk, Russia
[2] Institute of Chemistry and Chemical Technology, Federal Research Center KSC SB RAS, Russian Academy of Sciences, Krasnoyarsk, Russia
[3] Reshetnev Siberian State Aerospace University, Krasnoyarsk, Russia
[4] Research and Education Center „Functional Nanomaterials" Immanuel Kant Baltic Federal University, Kaliningrad, Russia
E-mail: baron@iph.krasn.ru

Received June 28, 2022
Revised August 19, 2022
Accepted September 3, 2022

The temperature dependence of the resistivity of titanium oxynitride TiN_xO_y thin films with different oxygen and nitrogen content obtained by atomic layer deposition was investigated. We found that the resistance of all films monotonically decreased with increasing temperature and varied within a wide range depending on the chemical composition and thickness of the film. The technology for obtaining a compact temperature sensor of wide range from helium to room temperature based on 40 nm thick $TiN_{0.87}O_{0.97}$ is presented.

Keywords: titanium oxide-nitride, temperature sensors, thin films, atomic layer deposition, integrated circuit components.

DOI: 10.21883/TPL.2022.10.54805.19292

Thin-film titanium oxynitride TiN_xO_y is used widely in various devices, such as integrated resistors [1], capacitors with a metal–insulator–metal structure (MIM capacitors) [2], photocatalysts [3,4], solar selective absorbers [5,6], and efficient photovoltaic energy converters [7]. The application of TiN_xO_y films as temperature sensors with a wide operating range is a new field of use of this material. Cernox^{TM} sensors based on zirconium oxynitride [8], carbon glasses, ruthenium oxide, and germanium tunnel diodes [9] are a well-known solution in this field. In the present study, we propose a novel method for fabrication of such sensors with the use of thin TiN_xO_y films fabricated by atomic layer deposition (ALD). The method of reactive magnetron sputtering is the one commonly used for titanium oxynitride synthesis [10]. However, ALD has an advantage in that it offers a considerably better thickness uniformity and a lower resistivity of grown films [7,11].

Films were grown in a SUNALE^{TM} R-200 ADVANCED (Picosun Oy, Finland) system without a load lock chamber at a temperature of 420°C. Two types of films with an increased ($G1$) and a reduced ($G2$) oxygen content were obtained. Liquid titanium tetrachloride ($TiCl_4$, 5N purity), gaseous ammonia (NH_3, 6N), and residual oxygen in the ALD chamber served as the sources of titanium, nitrogen, and oxygen, respectively. Sitall ST-32-1 plates with a thickness of 500 μm and (100) Si wafers ($\rho > 0.1\,k\Omega \cdot m$) with a thickness of 720 μm were used as substrates. $TiCl_4$ and NH_3 were fed periodically into the chamber in alternating 0.1- and 1-s-long pulses, respectively. In each deposition cycle, $TiCl_4$ was purged with a $2.5 \cdot 10^{-6}\,m^3 \cdot s^{-1}$ flow of nitrogen (7N) for 2 s, while NH_3 was purged with a flow of $1.7 \cdot 10^{-6} m^3 \cdot s^{-1}$ for 4 s. The base pressure was 500–700 Pa. The maximum pressure of $TiCl_4$ and NH_3 pulses was as high as 2500–3000 and 4000–4500 Pa, respectively. Prior to the growth of the studied TiN_xO_y film samples, the ALD reactor chamber was purged with pure nitrogen (8N), annealed at 420°C for 4 h, and passivated in 2000 cycles of TiN_xO_y growth at 420°C. The concentration of oxygen in films $G2$ was reduced by purging the ALD chamber with forming gas (FG) (N_2 (5N) : H_2(6N)=97 : 3) immediately before the start of the growth process. FG was supplied for 900 s in pulses with a duration of 15 s without purging with nitrogen. The process parameters of TiN_xO_y growth were detailed in [12].

The film thickness was measured with a Hitachi HT7700 transmission electron microscope (TEM) at a voltage of 100 kV and an emission current of 8 μA (Fig. 1, *a*). Figure 1 shows the TEM image of the $TiN_{0.55}O_{0.95}$ film cross section. The SiO_2 layer below $TiN_{0.55}O_{0.95}$ formed as a result of silicon oxidation in the process of loading a wafer into the hot ALD chamber and evacuation to the base vacuum. Roughness S_q (mean-square height) and the maximum level difference S_z of the obtained film texture was measured using atomic force microscopy (AFM) for samples type $G1$ and $G2$ (Figs. 1, *b*, *c*). The typical values of S_q for films $G1$ and $G2$ on sitall are 4.1 and 3.0 nm, and the values of S_z are 52 and 34 nm, respectively. Films grown on silicon have lower S_q (2.9 nm) and S_z (22 nm) values. TiN_xO_y films with a lower oxygen concentration have better-quality surfaces with a lower roughness.

The transport properties of films were determined using the four-probe method and a LakeShore EMPX-H2

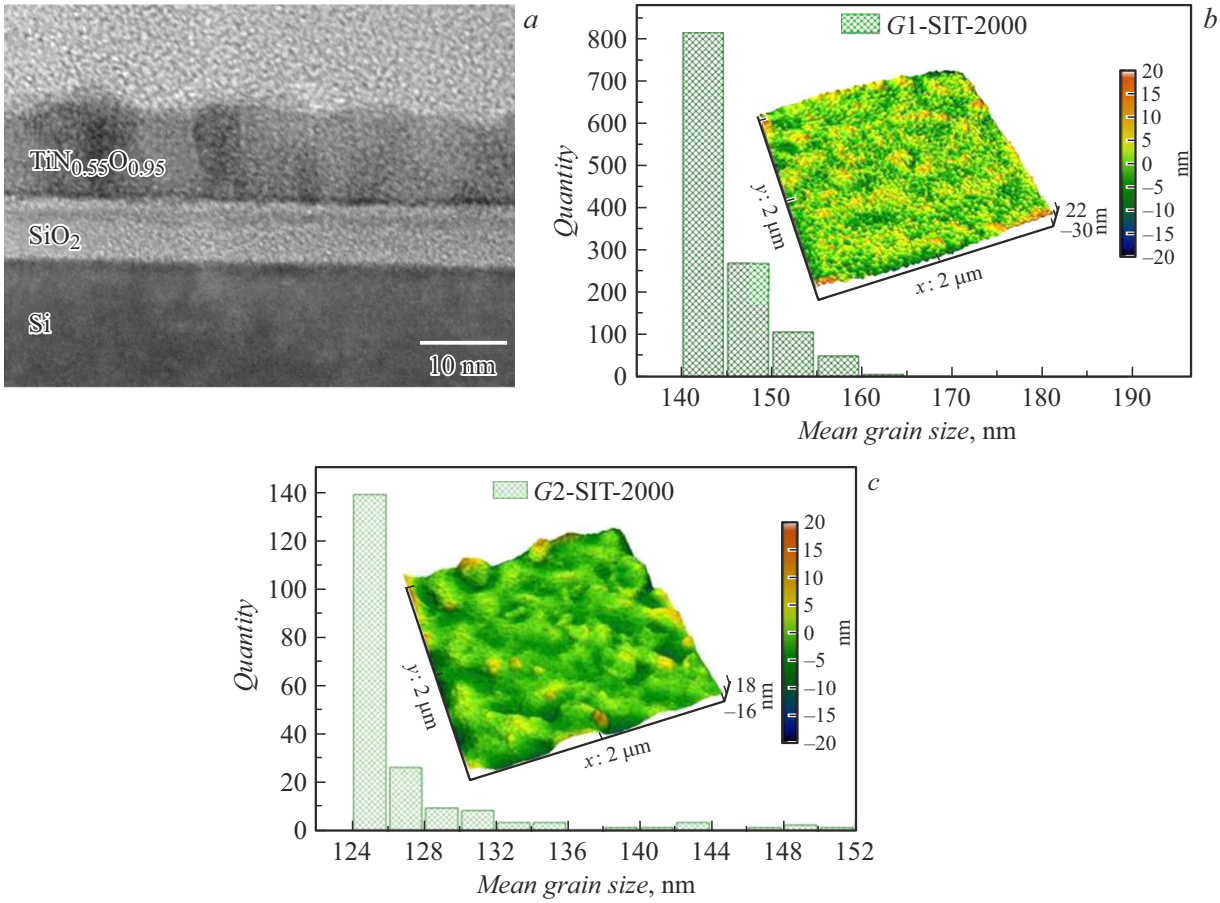

Figure 1. *a* — TEM image of sample *G*2-Si-638 of thin-film $TiN_{0.55}O_{0.95}$ on SiO_2/Si synthesized by ALD. *b*, *c* — AFM data for the surface of titanium oxynitride films on sitall and histograms of the grain size distribution: *b* — $TiN_{0.46}O_{1.52}$ with a high relative oxygen content, *c* — $TiN_{0.87}O_{0.97}$ with a low relative oxygen content.

Chemical composition and resistivity of TiN_xO_y films

Sample	Ti, at.%	N, at.%	O, at.%	Formula	Film thickness, nm	ρ, Ω · m (at 300 K)
*G*2-Si-638	40	22	38	$TiN_{0.55}O_{0.95}$	11	$7.8 \cdot 10^{-5}$
*G*1-Si-2000	33	16	51	$TiN_{0.48}O_{1.56}$	20	$(7.7 - 16) \cdot 10^{-4}$
*G*1-SIT-2000	34	15	51	$TiN_{0.46}O_{1.52}$	20	$(3.3 - 10) \cdot 10^{-4}$
*G*2-Si-4000	36	29	35	$TiN_{0.81}O_{0.98}$	90	$1.0 \cdot 10^{-5}$
*G*2-SIT-4000	35	31	34	$TiN_{0.87}O_{0.97}$	90	$9.0 \cdot 10^{-6}$

cryogenic probe station. Measurements were performed with a Kiethley 2634B dual-channel sourcemeter in the direct current mode. The temperature dependences of resistivity of TiN_xO_y films were obtained this way. The composition of films and the chemical state of elements were determined by X-ray photoelectron spectroscopy using a SPECS (Germany) spectrometer with a PHOIBOS 150 MCD 9 hemispherical analyzer; prior to these measurements, the surface was cleaned by ion etching. Data on the composition and resistivity of several typical samples are presented in the table. The sample designations contain the following information: oxygen concentration group (*G*1 or *G*2), substrate material (silicon or sitall), and number of ALD growth cycles. The chemical composition of films was determined more accurately in regard to the copper concentration by Rutherford backscattering of helium $^4He^+$ ions accelerated to 1.5 MeV in an AN2500 Van de Graaff accelerator produced by High Voltage Engineering Europa B.V. (Amersfoort, Netherlands). The obtained spectra were processed using the SIMNRA 7.03 program [13]. Although the FG supply line was fitted with a brass valve, TiN_xO_y films were not, in contrast to our previous experiments [12], contaminated with copper. The copper content did not exceed 0.02 at.%. The growth rate of *G*1 and *G*2 films was

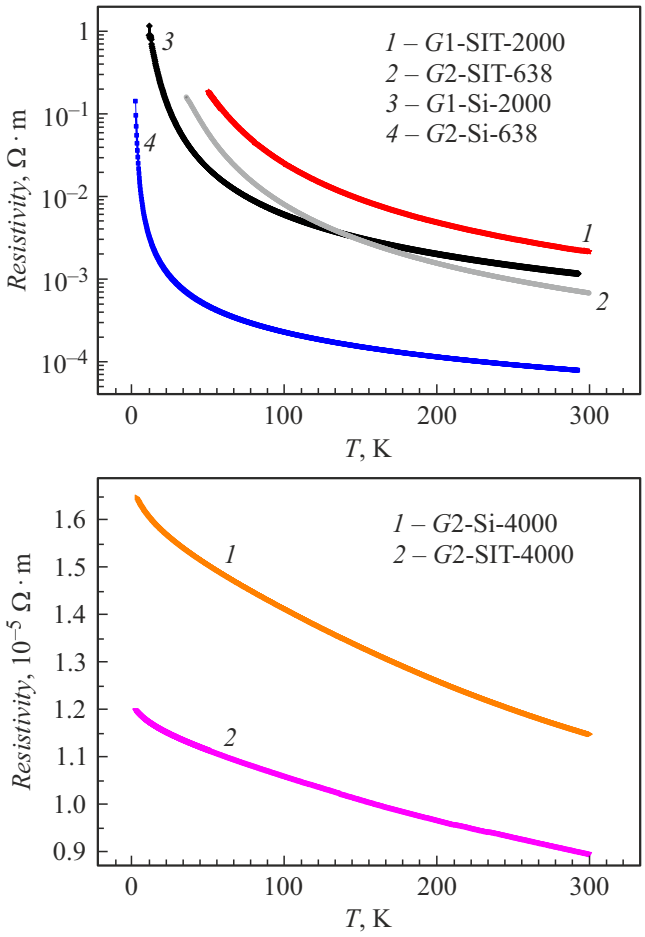

Figure 2. Temperature dependences of resistivity of TiN_xO_y films deposited by ALD onto sitall plates (SIT) and silicon wafers (Si). The oxygen-to-nitrogen ratio in samples $G1$ is 2–3 times higher than the corresponding ratio in samples $G2$. Numbers in designations correspond to the total number of ALD growth cycles.

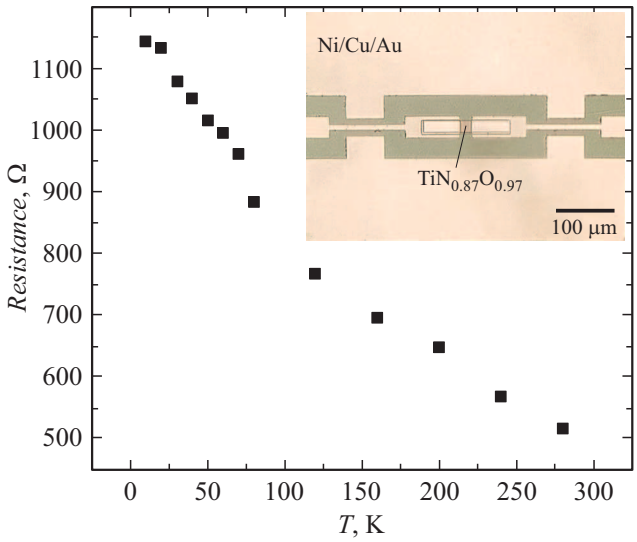

Figure 3. Temperature dependence of resistance and photomicrograph (inset) of the sensor based on a $TiN_{0.87}O_{0.97}$ film with a thickness of 40 nm.

0.11 Å/cycle and 0.22 Å/cycle, respectively. The film growth rate decreases significantly when the oxygen concentration in the chamber increases.

Figure 2 presents the temperature dependences of resistivity of the studied TiN_xO_y films. All samples exhibit a strictly monotonic dependence of resistivity, which decreases with increasing temperature. The results of measurements at above-room temperature revealed that this monotonic resistivity reduction continues up to 260°C. At higher temperatures, the resistivity of group $G1$ films increases abruptly and irreversibly. Films $G1$ have a roughly inverse quadratic dependence on temperature, while the dependence for films $G2$ is hyperbolic. The range of resistivity variation depends on the thickness of films, the oxygen content, and the substrate roughness. It should be noted that films grown on a silicon substrate have a stronger temperature dependence in the low-temperature region. This is probably attributable to the difference in size of crystallites in films on silicon and sitall substrates (Fig. 1). Having analyzed the histograms of crystallite size distributions, we found that the mean size of grains in films grown on sitall substrates is 140 nm for samples $G1$ and 120 nm for samples $G2$, while the corresponding value for samples $G1$ on silicon is 155 nm. The substrate roughness has a significant influence on resistivity (with the difference being as high as an order of magnitude) of thin films (11 nm), but has a less pronounced effect (50–100% resistivity difference) in thick films (90 nm). Roughness S_q of the initial substrates determined based on AFM data was 0.28 nm for silicon and 16.76 nm for sitall. An increase (reduction) in oxygen (nitrogen) content and a reduction in the film thickness contribute to a significant (1–2 orders of magnitude) increase in resistivity. Indeed, it follows from the table that samples $G2$-Si-638 and $G2$-Si-4000 have very close oxygen concentrations, but differ in thickness by a factor of ~ 8.2, which is roughly equal to the inverse ratio of their resistivities (~ 7.8). Comparing samples $G2$-Si-4000 and $G2$-SIT-4000 with the same film thickness and different oxygen content, one also finds that a 1% reduction in oxygen concentration translates into a 10% reduction in resistivity.

Figure 3 presents the temperature dependence of resistance and the photomicrograph of a typical TiN_xO_y sensor with interconnections and contact pads with a gold coating. The body of this sensor was formed from a low-resistivity $G2$ $TiN_{0.87}O_{0.97}$ film with a thickness of 40 nm deposited onto sitall. The process of fabrication of this structure has been illustrated earlier through an example of resistive elements based on a $G1$ $TiN_{0.82}O_{1.43}$ film [14]. The active region (body) of the sensor was formed from a $TiN_{0.87}O_{0.97}$ film by optical lithography in an EVG 610 setup with subsequent plasma etching in a RIE-1701 Nordson MARCH system in a CF_4 ($2.5 \cdot 10^{-7} m^3 \cdot s^{-1}$)/$O_2$ ($5 \cdot 10^{-8} m^3 \cdot s^{-1}$) gas mixture at a high-frequency power of 250 W and a pressure 33 Pa for 120 s. Electric contacts and

interconnections were formed as a second overlapping layer by optical lithography with the use of an AZ nLOF-2035 negative photoresist and electron beam deposition of Ni (5 nm)/Cu (1 μm)/Ni (5 nm)/Au (50 nm) with subsequent lift-off stripping in acetone.

This method of fabrication of temperature sensors provides an opportunity to adjust their resistance within a wide range (0.01−100 kΩ) by controlling accurately the thickness of TiN_xO_y in the process of ALD growth and the geometric size of the structure in lithography and by varying the oxygen content. We plan to establish control over the oxygen concentration parameter in the future. The sensor fabrication process is based on standard silicon microelectronics technology, and the obtained sensor itself is easy to integrate into modern microchips.

Acknowledgments

The authors express their gratitude to the Krasnoyarsk Regional Resource Sharing Center of the Krasnoyarsk Science Center (Siberian Branch, Russian Academy of Sciences) for providing the needed equipment.

Funding

This study was supported financially by the Russian Foundation for Basic Research, the Government of Krasnoyarsk Krai, and the Krasnoyarsk Krai Foundation of Science as part of scientific project No. 20-42-240013. The Rutherford backscattering study of samples was performed at Research and Education Center „Functional Nanomaterials“ of the Baltic Federal University with financial support from the Ministry of Science and Higher Education of the Russian Federation (project FZWN-2020-0008).

Conflict of interest

The authors declare that they have no conflict of interest.

References

[1] N.D. Cuong, D.J. Kim, B.D. Kang, S.G.J. Yoon, Electrochem. Soc., **153**, G856 (2006). DOI: 10.1149/1.2219707
[2] S. Iwashita, S. Aoyama, M. Nasu, K. Shimomura, N. Noro, T. Hasegawa, Y. Akasaka, K. Miyashita, J. Vac. Sci. Technol. A, **34**, 01A145 (2016). DOI: 10.1116/1.4938106
[3] R. Asahi, T. Morikawa, T. Ohwaki, K. Aoki, Y. Taga, Science, **293**, 269 (2001). DOI: 10.1126/science.1061051
[4] E. Martinez-Ferrero, Y. Sakatani, C. Boissiere, D. Grosso, A. Fuertes, J. Fraxedas, C. Sanchez, Adv. Funct. Mater., **17**, 3348 (2007). DOI: 10.1002/adfm.200700396
[5] M. Lazarov, P. Raths, H. Metzger, W. Spirkl, J. Appl. Phys., **77**, 2133 (1995). DOI: 10.1063/1.358790
[6] A. Rizzo, M.A. Signore, L. Tapfer, E. Piscopiello, A. Cappello, E. Bemporad, M. Sebastiani, J. Phys. D: Appl. Phys., **42**, 115406 (2009). DOI: 10.1088/0022-3727/42/11/115406
[7] X. Yang, Y. Lin, J. Liu, W. Liu, Q. Bi, X. Song, J. Kang, F. Xu, L. Xu, M.N. Hedhili, D. Baran, X. Zhang, T.D. Anthopoulos, S. De Wolf, Adv. Mater., **32**, 2002608 (2020). DOI: 10.1002/adma.202002608
[8] S.S. Courts, P.R. Swinehart, AIP Conf. Proc., **684**, 393(2003). DOI: 10.1063/1.1627157
[9] C.J. Yeager, S.S. Courts, IEEE Sensors J., **1**, 352 (2001). DOI: 10.1109/7361.983476
[10] E.S. Kiseleva, *Fiziko-mekhanicheskie svoistva i struktura plenok dioksida i oksinitrida titana, osazhdennykh metodom reaktivnogo magnetronnogo raspyleniya*, Candidate's Dissertation in Mathematics and Physics (Nats. Issled. Tomsk. Politekh. Univ., Tomsk, 2016) (in Russian).
[11] J.-M. Chappé, N. Martin, J. Lintymer, F. Sthal, G. Terwagne, J. Takadoum, Appl. Surf. Sci., **253**, 5312 (2007). DOI: 10.1016/j.apsusc.2006.12.004
[12] F.A. Baron, Y.L. Mikhlin, M.S. Molokeev, M.V. Rautskiy, I.A. Tarasov, M.N. Volochaev, L.V. Shanidze, A.V. Lukyanenko, T.E. Smolyarova, S.O. Konovalov, F.V. Zelenov, A.S. Tarasov, N.V. Volkov, ACS Appl. Mater. Interfaces, **13**, 32531 (2021). DOI: 10.1021/acsami.1c08036
[13] M. Mayer, AIP Conf. Proc., **475**, 541 (1999). DOI: 10.1063/1.59188
[14] L.V. Shanidze, A.S. Tarasov, M.V. Rautskiy, F.V. Zelenov, S.O. Konovalov, I.V. Nemtsev, A.S. Voloshin, I.A. Tarasov, F.A. Baron, N.V. Volkov, Appl. Sci., **11**, 7498 (2021). DOI: 10.3390/app11167498